ELSEVIER

Catalysis Today 67 (2001) 151–157

CATALYSIS TODAY

www.elsevier.com/locate/cattod

Butane partial oxidation in an externally fluidized bed-membrane reactor

M. Alonso [a], M.J. Lorences [a], M.P. Pina [b], G.S. Patience [c,*]

[a] *Department of Chemical Engineering and Environmental Technology, University of Oviedo, 33007 Oviedo, Spain*

[b] *Department of Chemical and Environmental Engineering, University of Zaragoza, 50009 Zaragoza, Spain*

[c] *Lycra®/Terathane®, DuPont International, Geneva, Switzerland*

Abstract

An externally fluidized bed-membrane reactor (EFBMR) for partial oxidation reactions is described. This novel reactor concept combines the advantages of fixed bed and fluid bed reactors. Catalyst is loaded inside a porous membrane tube into which the hydrocarbon is fed. An oxygen rich gas fluidizes a powder on the shell side. Oxygen crosses the membrane wall and reacts. Butane partial oxidation to maleic anhydride was adopted as the model reaction and the kinetic parameters were derived based on a full scale commercial pilot plant. A detailed reaction engineering model of the EFBMR showed that hot spots are minimized and the reactor is inherently safer because the flammability potential is lower. Maleic yields are potentially 50% higher in an EFBMR compared to a conventional fixed bed reactor and the reactant concentration operating range is much wider.

Keywords: Membrane reactor; Fluid bed; Butane oxidation; Maleic anhydride; VPO catalyst

1. Introduction

Maleic anhydride is a multi-functional compound and is an important precursor to various non-saturated polyether resins. Over the last few decades, its manufacture base has shifted from benzene to butane as the preferred feed stock. It is produced in fixed beds, fluid beds and in transport bed reactors [1]. In this paper, we simulate a new reactor concept that is based on combining the advantages of the fixed and fluid bed reactors and we have designated it as the externally fluidized bed-membrane reactor (EFBMR). Butane is fed to a fixed bed of catalyst contained in a sintered porous (metal or ceramic) membrane tube and oxygen crosses the membrane wall from an externally fluidized bed as shown in Fig. 1. Several applications of inert membrane reactors are described in the literature [2]. They are recognized as inherently safe contacting device for gas phase oxidation of hydrocarbons, particularly with respect to process control and hazards minimization [3].

In order to evaluate the potential of an EFBMR, we compared published experimental data from a full scale pilot plant [4] and calculations of the EFBMR performance with a similar geometry using a detailed reaction engineering model. The commercial configuration together with the thousands of porous metal (or ceramic) tubes would also contain cooling coils in

* Corresponding author. Fax: +41-22-717-6868.
E-mail address: gregory.patience@che.dupont.com (G.S. Patience).

0920-5861/01/$ – see front matter
PII: S0920-5861(01)00307-8

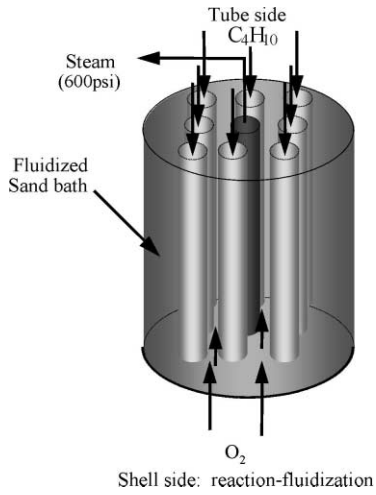

Fig. 1. Schematic diagram for an externally fluidized bed-membrane reactor (EFBMR).

the fluid bed. The fluid bed maintains the reactor in isothermal conditions and provides an efficient means to generate steam.

2. Reactor model

2.1. Kinetics of butane partial oxidation over VPO catalyst

The partial oxidation of *n*-butane to maleic anhydride over vanadium phosphorous oxide (VPO) catalyst is one of the most complex heterogeneously catalyzed reactions practiced industrially. VPO is unique with respect to its ability to selectively transform alkanes to oxygenated products at low temperatures with yields of up to 60% [5]. The selective phase — V^{5+} — is distributed on the surface and the bulk is vanadyl pyrophosphate matrix [6,7]. The catalyst is synthesized in both aqueous and organic medium. The latter preparation method generally results in a more selective catalyst with a higher surface area, whereas the former produces a more active catalyst. The active phase changes as a function of the reducing or oxidizing environment, water concentration [8,9], time on stream [10,11] and reaction temperature.

Both maleic anhydride and *n*-butane compete for oxygenated sites and may be oxidized to CO and CO_2, as shown in Fig. 2, where r_1 corresponds to the

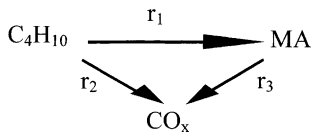

Fig. 2. Reaction network for butane partial oxidation.

maleic anhydride formation rate from butane, r_2 corresponds to the carbon oxides (CO, CO_2) formation rate from butane and r_3 corresponds to the carbon oxides formation rate from maleic anhydride. Although byproduct acids are also detected in the product stream (acetic acid, acrylic acid and small quantities of phthalic and methacrylic acid), their contribution to the general reaction scheme is considered negligible (concentrations lower than 2%).

Both Langmuir–Hinshelwood models [12,13] and redox models [14–17] have been proposed to characterize the reaction kinetics. Based on pulsing and oxygen isotope labeling studies [18] in which a hydrocarbon rich stream is fed to a previously oxygen treated catalyst, VPO can store as much as 100 mmol of oxygen/kg of catalyst. Thus, it would appear that the Mars van Krevelen model best approximates the reaction mechanism, *n*-butane reacts with catalyst lattice oxygen and thus reduces the active vanadium site from a 5^+ to a 4^+ valence.

Although V^{3+} sites have also been reported in the literature [14], this phase is only significant when the catalyst becomes highly reduced. In this paper, we adopt a two step redox model with product inhibition [15] to characterize the reaction rates, r_j (kmol/s kg):

$$r_j = \frac{k_j C_4}{1 + K_1 C_4/O_2 + K_2 MA/O_2}, \qquad j = 1, 2 \quad (1)$$

$$r_3 = \frac{k_3 MA}{1 + K_1 C_4/O_2 + K_2 MA/O_2}, \qquad j = 3 \quad (2)$$

where C_4, MA, O_2 are the butane, maleic anhydride and oxygen concentrations (kmol/m^3), respectively, K_1 and K_2 are the inhibition factors and the Arrhenius type kinetic constants, k_j, are calculated based on a normalized reference temperature of 653 K:

$$k_j = k_{j,653} \exp\left[\frac{-Ea_j}{R}\left(\frac{1}{T} - \frac{1}{653}\right)\right], \quad j = 1, 2, 3 \quad (3)$$

where Ea_j is the activation energy for jth reaction (kJ/mol), T the reaction temperature (K) and R is the gas constant (8.314×10^{-3} kJ/mol K).

2.2. Reactor equations and kinetic parameters estimation

In order to estimate the kinetic parameters (k_j, Ea_j, and K), we developed a reaction engineering model based on a commercial scale pilot plant data published by Sharma et al. [4]. The kinetic data — see Table 2 and Fig. 3 — were collected in a 25 mm diameter fixed bed 5 m long containing approximately 2 kg of 3 mm extrudates of a commercial promoted VPO catalyst [4].

The engineering model assumes the flow domain to be one-dimensional so that radial temperature and concentration gradients are ignored. Under steady-state conditions, the mass conservation equation for the ith species in a differential reactor volume results in

$$\frac{dF_i}{dz} - N_i\frac{4}{d} + \sum_{j=1}^{7} a_{ij}\eta_j r_j \rho_s(1-\varepsilon) = 0 \tag{4}$$

where F_i is the axial molar flow rate per unit of cross-sectional area of component "i" in kmol/m^2 s, N_i is the permeation rate in kmol/m^2 s for the ith species that permeates across the membrane wall (it equals 0 for a fixed bed), d the membrane diameter, a_{ij} parameter the stoichiometric coefficient for the ith species in the jth reaction, which is positive for reactants and negative for products, η_j is the effectiveness factor and r_j is the rate of products formation in kmol/kg s, $\rho_s(1-\varepsilon)$ represents the mass of catalyst inside the membrane.

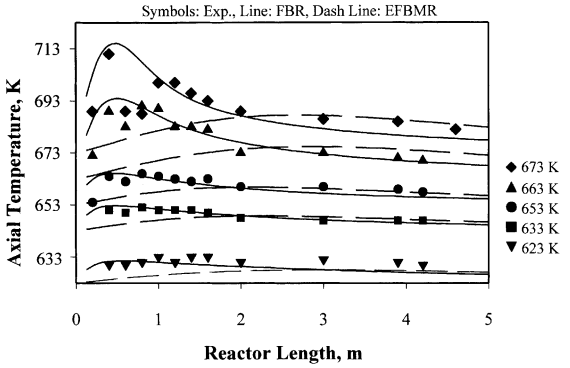

Fig. 3. Temperature profiles along the reactor for the inlet conditions summarized in Table 2: (A) experimental results of Sharma et al. [4]; (B) FBR model predictions; (C) EFBMR model predictions.

The energy balance for the reactor is

$$\frac{d(FTC_p)}{dz} - \sum_{i=1}^{n} N_i\frac{4}{d}C_{P,i}(T_{bath} - T_{ref}) + U_{ov}\frac{4}{d}(T - T_{bath}) - \sum_{j=1}^{7}(-\Delta H_j)\eta_{(j)}r_{(j)}\rho_s(1-\varepsilon) = 0 \tag{5}$$

where U_{ov} is the overall heat transfer coefficient, T_{bath} is the fluid bed or molten salt bath temperature and $C_{p,g}$ represents the heat capacity. As in the case of the material balance equation, the second term in the energy balance equation equals zero for a fixed bed. The pressure drop across the catalyst is calculated based on the Ergun equation:

$$\frac{\Delta P}{\Delta z} - 150\frac{(1-\varepsilon)^2}{\varepsilon^3}\frac{\mu}{d_p^2}U_g - 1.75\frac{(1-\varepsilon)}{\varepsilon^3}\frac{\rho}{d_p}U_g^2 = 0 \tag{6}$$

where ΔP is the pressure drop, U_g the gas velocity, d_p the particle diameter, ε is the void fraction, and μ and ρ are the fluid viscosity and density, respectively. The model assumes that the diffusion resistance of the pellets is negligible. The material and energy balance equations were discretized according to the volume element formulation and solved simultaneously using a Newton–Raphson iteration scheme. After each iteration, the pressure profile was calculated by the Ergun equation.

The three rate constants and activation energies — Table 1 — were calculated by minimizing the following object function:

$$\Phi = 2 - R^2_{X_{C_4H_{10}}} - R^2_{S_{MA}} \tag{7}$$

with

$$R^2_{X_{C_4H_{10}}} = 1 - \frac{\sum(X_{C_4H_{10},calc} - X_{C_4H_{10},exp})^2}{\sum(X_{C_4H_{10},exp} - \bar{X}_{C_4H_{10},exp})^2},$$

$$R^2_{S_{MA}} = 1 - \frac{\sum(S_{MA,calc} - S_{MA,exp})^2}{\sum(S_{MA,exp} - \bar{S}_{MA,exp})^2},$$

Table 1
Kinetic parameters comparison

	$VPO_{1.0}$[a]	$VPO_{1.1}$[a]	VPO[b]
$k_{1,653\,K}$ (s^{-1})	1.96	0.61	0.86
$k_{2,653\,K}$ (s^{-1})	0.86	0.3	0.11
$k_{3,653\,K}$ (s^{-1})	0.07	0.04	0.19
Ea_1 (kJ/mol)	125	116	80
Ea_2 (kJ/mol)	145	130	80
Ea_3 (kJ/mol)	180	138	98
K_1	59	20	20
K_2	26	12	12

[a] Kinetic parameters obtained by Buchanan and Sundaresan [15].
[b] Kinetic parameters obtained in this work from the experimental data of Sharma et al. [4].

where R^2 represents the coefficient of multiple determination, $X_{C_4H_{10}}$ is the butane conversion and S_{MA} is the maleic anhydride selectivity.

Kinetic parameters for a catalyst with a *P/V* ratio of 1 and 1.1 obtained in a laboratory-scale reactor by Buchanan and Sundaresan [15] are compared in Table 1 with the values estimated from the pilot plant experimental data. Catalyst with excess phosphorous ($VPO_{1.1}$) is less active and has a lower surface area compared to the catalyst with a *P/V* ratio equal to 1. The adsorption coefficient, *K*, is also higher for $VPO_{1.0}$ catalyst. The commercially "equilibrated" catalyst has the lowest surface area, and the estimated activation energies are significantly lower than those reported by the cited authors. These discrepancies may be attributed to the different catalyst preparation routes employed. Similar activation energies for VPO catalyst prepared in an aqueous medium are reported in the literature [19]. The rate constant for maleic anhydride decomposition, k_3, is also higher for the commercial catalyst (i.e. a catalyst more active but less selective).

The reaction engineering model fits the experimental data very well as shown in Table 2. It accounts for 99.6% of variance in conversion. Fig. 3 shows a reasonable agreement between the measured and the predicted temperature profile. Moreover, the proposed two-site kinetic model fits the experimental data better compared to the adsorption model [4].

3. Results and discussion

3.1. Model predictions

Fig. 3 illustrates the calculated temperature profile for the pilot plant reactor and a externally fluidized bed-membrane reactor at the same operating conditions and inlet gas composition. The experimental plant data [4] are also plotted and agreement between the reaction engineering model and data is remarkable. In the pilot plant, temperature was controlled by a molten salt bath whereas, the heat transfer medium in the EFBMR is a fluid bed. At low temperatures,

Table 2
Comparative table of experimental results and model predictions

Feed (Nm^3/h)	1.68	1.68	1.65	1.65	1.66
$C_4H_{10,inlet}$ (%)	1.82	1.86	0.75	0.75	1.26
T_{bath} (°C)	400	390	380	370	350
Hot spot (°C)[a]					
1	440	419	392	380	360
2	451	424	393	380	359
3	442	420	393	380	359
Conversion[a]					
1	90	84	89	81	52
2	91	77	82	72	42
3	91	84	88	81	55
Selectivity[a]					
1	60	68	66	72	82
2	58	63	71	72	74
3	59	67	66	73	81

[a] 1: Experimental data from Sharma et al. [4]; 2: model predictions of Sharma et al. [4]; 3: the reaction engineering FBR model predictions.

both reactors show near isothermal behavior and the temperature difference between the cooling medium (molten salt bath or fluid bed) is no more than about 10°C. At higher molten salt temperatures, reaction rates increase together with MA production, however, the temperature profile is no longer flat and a hot spot develops at about 0.5 m from the gas inlet. On the contrary, the EFBMR temperature profile remains relatively flat. For example, when the molten salt temperature is 400°C, the hot spot in the fixed bed is in the order of 40°C, it is only 15°C in the EFBMR. The hot spot temperature is a limiting factor with respect to achieving high product yields due to runaway, in which the reaction becomes uncontrollable.

3.2. Safety aspects and reactor operability: FBR vs. EFBMR

The hot spot temperature is one of the several factors constraining the operating range — pressure, temperature, flow rate — and feed gas composition. Two other constraints include the butane/oxygen flammability limits and the maximum temperature. The rate of phosphorous depletion increases with temperature. In order to maintain catalyst stability, commercial reactors typically operate at temperatures below 440–450°C. In this study, we consider the upper temperature limit to be 440°C. Fig. 4 illustrates the flammability region for butane and oxygen mixtures. Generally, fixed bed reactors operate in the range of 2% butane in air, although some commercial manufactures are exploring the high butane and lower oxygen concentrations — 9% butane and 10% oxygen, for example. The operating range with respect to butane/oxygen concentrations is higher in an EFBMR because the reactants are mixed in the presence of solids. The fixed bed of catalyst acts as an efficient flame arrestor and thus the possibility of flame propagation is very low in the bed. The greatest risk for deflagration is in the plenum chamber upstream of the bed where butane and air are mixed or downstream of the catalyst.

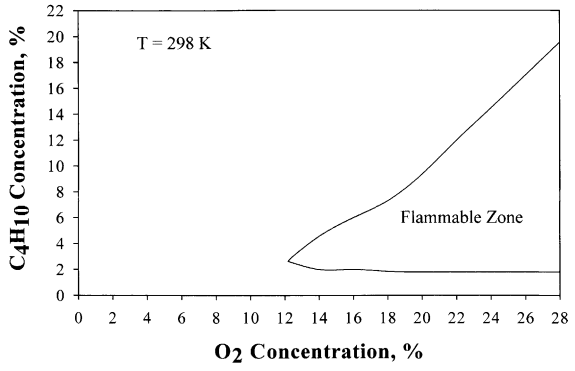

Fig. 4. Flammability chart for butane/oxygen mixtures at 298 K and atmospheric pressure.

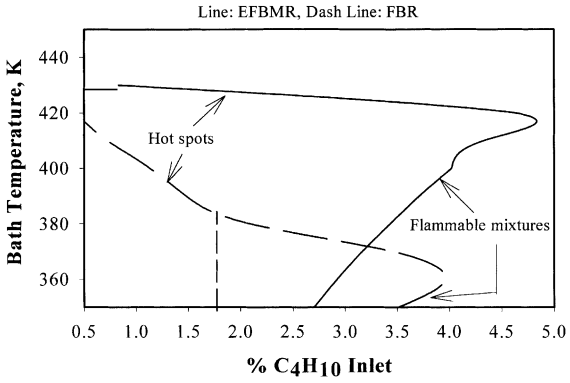

Fig. 5. Stable operating range for an FBR (butane + enriched air) and an EFBMR (butane + nitrogen in the tube side/pure oxygen in the shell side). Total flow rate: 0.95 Nm^3/h, bath temperature and butane inlet concentration as variables.

Fig. 5 compares the stable operating temperature and butane concentration for an EFBMR and an FBR also immersed in a similar fluid bed. The range for an EFBMR is larger and this is due to both the flammability constraints as well as runaway reaction. We considered a 40°C temperature difference between the cooling media and the fixed bed temperature as the demarcation between stable operation and runaway. The dashed line in the figure represents the stability limit for a fixed bed at different butane concentrations in enriched air. Note that the vertical line at 1.8% butane represents the flammability limit, the region to the right is stable with respect to runaway but not with respect to flammability.

The maximum butane limit for an EFBMR decreases with decreasing temperature and is due to the butane/oxygen composition at the exit of the reactor: butane conversion drops as the temperature decreases and thus the exit butane concentration rises above 1.8%. At temperatures between 410 and 420°C, the butane conversion approaches 70%, so it

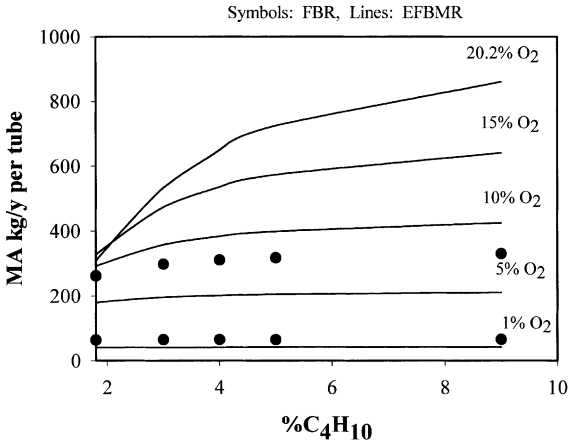

Fig. 6. MA production per tube in an EFBMR (butane + nitrogen in the tube side/pure oxygen in the shell side) and FBR at 420°C and 0.95 Nm^3/h, butane and oxygen concentration as variables.

would be possible to operate safely with butane inlet concentrations as high as 4.5%.

Fig. 6 represents the MA production rate in kg/year/tube as a function of butane and oxygen concentration at a bath temperature of 420°C for both reactor types. The total inlet molar flow rate was constant for all cases. Production increases almost linearly with $\%O_2$ at high butane concentrations. It is less sensitive to oxygen at low butane concentrations. Under typical fixed bed conditions — 2% butane in air — MA production in an FBR is higher than in an EFBMR. The advantage of the EFBMR compared to the fixed bed is evident only at the high butane and oxygen concentrations. Besides the limitation with respect to flammability, the fixed bed reactor cases were restricted due to the hot spot stability criteria. For example, with 10% oxygen and 4% butane, the temperature in the bed rose to well over 440°C.

The gas composition and temperature profiles along the EFBMR with 9% C_4H_{10} and 20% O_2 in the feed (Fig. 6) are demonstrated in Fig. 7. The temperature rises gradually at the entrance and approaches a maximum value and remains constant, which is quite different than the classical fixed bed hot spot pattern (Fig. 3). This may imply that even longer tubes could improve maleic production because the maleic concentration increases almost linearly with tube length. Note, however, that the oxygen concentration also increases with tube length and its exit concentration could be a limiting factor. An important consideration is the auto-ignition temperature (AIT) of the mixture, which is the lowest temperature at which a given gas mixture self-ignites. It depends on pressure, geometry and gas composition and is in the order of 300°C for butane in air. In order to operate the reactor safely, the exit temperature should be below the AIT and the exit oxygen concentrations should be lowerd Otherwise, specialized operations are required to bring the gas temperature below the AIT.

Note that the kinetic parameters were derived for highly oxidizing reaction conditions. The projections of reactor performance under reducing conditions serve to illustrate the expected trend and to

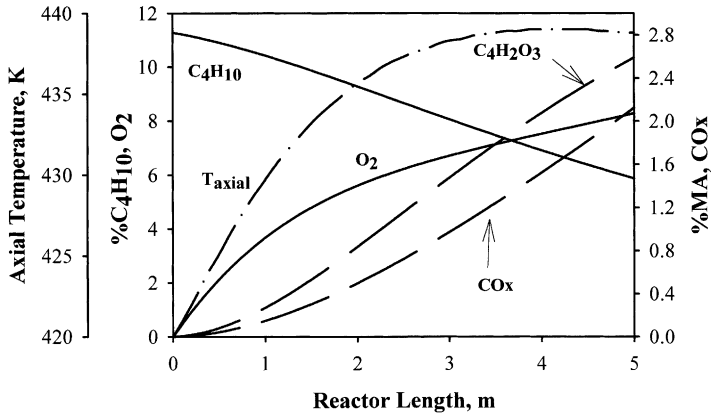

Fig. 7. Temperature and product concentration profiles along the EFBMR (T_{bath} = 420°C, 0.95 Nm^3/h, butane + nitrogen in the tube side/pure oxygen in the shell side, 9% C_4H_{10}, 20% O_2).

compare the performance between the two reactor types. Kinetic experiments under reducing conditions are required in order to evaluate the commercial potential of the EFBMR.

4. Conclusions

An EFBMR offers several advantages over the fixed bed technology for partial oxidation reactions, particularly reactions that are highly exothermic. They provide a wider operating range with respect to both temperature and inlet gas composition. Furthermore, they are inherently safer since the hydrocarbon and oxidant are mixed in the presence of solids, which are efficient flame arrestors. The higher butane concentrations and controlled addition of oxygen along the reactor length by means of a membrane lead to higher product rates if the heat removal scheme keeps the controllability of the overall system.

Herein, we applied a two-site kinetic model [15] and successfully characterized performance of a commercial scale fixed bed pilot reactor for the oxidation of butane to maleic anhydride [4]. The reactor engineering model fits both the concentration and temperature profile along the reactor length very well. We then integrated the reaction kinetics into an EFBMR model and demonstrated that potential production rates with this reactor configuration is more than 50% higher than a fixed bed.

References

[1] R.M. Contractor, D.I. Garnett, H.S. Horowitz, H.E. Bergna, G.S. Patience, J.T. Schwartz, G.M. Sisler, in: V. Cortés, S. Vic (Eds.), New Developments in Selective Oxidation II, Vol. 82, Elsevier, New York, 1994, p. 233 (Chap. 3).
[2] H.P. Hsieh, Inorganic Membranes for Separation and Reaction, Elsevier , Amsterdam, 1996.
[3] J. Coronas, M. Menéndez, J. Santamaría, J. Loss. Prev. Process Ind. 8 (2) (1995) 97.
[4] R.K. Sharma, D.L. Creswell, E.J. Newson, AIChE J. 37 (1) (1991) 39.
[5] J.C. Burnett, R.A. Keppel, W.D. Robinson, Catal. Today 1 (5) (1987) 537.
[6] B.K. Hodnett, Catal. Today 1 (1987) 477.
[7] E. Bordes, Catal. Today 1 (1987) 499.
[8] E.W. Arnold, S. Sundaresan, Appl. Catal. 41 (1988) 225.
[9] H.W. Zanthoff, M. Sananes-Schultz, S.A. Buchholz, U. Rodemerck, B. Kubias, M. Baerns, Appl. Catal. A 172 (1998) 49.
[10] W. Partenheimer, B.L. Meyers, Appl. Catal. 51 (1989) 13.
[11] G. Centi, F. Trifiro, G. Busca, J.R. Ebner, J.T. Gleaves, Faraday Discuss. Chem. Soc. 87 (1989) 215.
[12] G. Centi, G. Fornasari, F. Trifiro, Ind. Eng. Chem. Prod. Res. Dev. 24 (1985) 32.
[13] J.J. Lerou, P.L. Mills, in: M.P.C. Weijnen, A.A.H. Drinkenburg (Eds.), Precision Process Technology, Kluwer Academic Publishers, Dordrecht, 1993, p. 175.
[14] G. Centi, G. Fornasari, F. Trifiro, J. Catal. 89 (1984) 44.
[15] J.S. Buchanan, S. Sundaresan, Appl. Catal. 26 (1986) 211.
[16] S.K. Bej, M.S. Rao, Ind. Eng. Chem. Res. 30 (1991) 1824.
[17] S.K. Bej, M.S. Rao, Ind. Eng. Chem. Res. 31 (1992) 2075.
[18] M.A. Pepera, J.L. Callahan, M.J. Desmond, E.C. Milberger, P.R. Blum, N.J. Bremer, J. Am. Chem. Soc. 107 (1985) 4883.
[19] P. Schneider, G. Emig, H. Hofmann, Ind. Eng. Chem. Res. 26 (1987) 2236.